PROTEINS
STRUCTURE ■ FUNCTION ■ BIOINFORMATICS

Structure of the ribosome associating GTPase HflX

Hao Wu,[1,2,3,†] Lei Sun,[1,2,†] Fabian Blombach,[1,†] Stan J. J. Brouns,[1] Ambrosius P. L. Snijders,[4] Kristina Lorenzen,[5] Robert H. H. van den Heuvel,[5] Albert J. R. Heck,[5] Sheng Fu,[2] Xuemei Li,[2] Xuejun C. Zhang,[2,3] Zihe Rao,[2] and John van der Oost[1*]

[1] Laboratory of Microbiology, Wageningen University, Wageningen, The Netherlands
[2] National Laboratory of Biomacromolecules, Institute of Biophysics, Chinese Academy of Sciences, Beijing, China
[3] Protein Studies Research Program, Oklahoma Medical Research Foundation, Oklahoma City, Oklahoma
[4] Department of Chemical and Process Engineering, University of Sheffield, Sheffield S1 3JD, UK
[5] Department of Biomolecular Mass Spectrometry, Utrecht University, Utrecht, The Netherlands

ABSTRACT

The HflX-family is a widely distributed but poorly characterized family of translation factor-related guanosine triphosphatases (GTPases) that interact with the large ribosomal subunit. This study describes the crystal structure of HflX from *Sulfolobus solfataricus* solved to 2.0-Å resolution in apo- and GDP-bound forms. The enzyme displays a two-domain architecture with a novel "HflX domain" at the N-terminus, and a classical G-domain at the C-terminus. The HflX domain is composed of a four-stranded parallel β-sheet flanked by two α-helices on either side, and an anti-parallel coiled coil of two long α-helices that lead to the G-domain. The cleft between the two domains accommodates the nucleotide binding site as well as the switch II region, which mediates interactions between the two domains. Conformational changes of the switch regions are therefore anticipated to reposition the HflX-domain upon GTP-binding. Slow GTPase activity has been confirmed, with an HflX domain deletion mutant exhibiting a 24-fold enhanced turnover rate, suggesting a regulatory role for the HflX domain. The conserved positively charged surface patches of the HflX-domain may mediate interaction with the large ribosomal subunit. The present study provides a structural basis to uncover the functional role of this GTPases family whose function is largely unknown.

Proteins 2010; 78:705–713.

Key words: HflX; sulfolobus; archaea; multi-domain GTPases.

INTRODUCTION

The P-loop guanosine triphosphatases (GTPases) control a multitude of biological processes, ranging from cell division, cell cycling, and signal transduction, to ribosome assembly and protein synthesis.[1–5] GTPases exert their control by interchanging between an inactive GDP-bound state and an active GTP-bound state, thereby acting as molecular switches.[6]

Within the Translation factor (TRAFAC) related class of P-loop GTPases, the HflX-type is a relatively unexplored family.[3] The broad phylogenetic distribution pattern of HflX GTPases in Bacteria, Archaea, and Eukaryotes (including human[7]) suggests a basic cellular function for this protein family.[5] The archetype *hflX* gene was originally found in *Escherichia coli* operon *hflA* (high frequency of lysogenization), and thought to be associated with the lytic–lysogenic decision of bacteriophage Lambda.[8] However, such a role for HflX was recently dismissed.[9] *E. coli* HflX as well as its homologue from *Chlamydophila pneumoniae* were shown to associate with large ribosomal subunits.[10,11] A model was proposed in which HflX recruits other factors to the large ribosomal subunit that play a direct role in ribosome assembly.[10] This model remains to be experimentally verified. Association with ribosomal subunits has been observed for many other GTPases such as Era,[12,13] Obg,[14,15] YlqF,[16] and YsxC,[17,18] which are thought to play a role in ribosome assembly. While the aforementioned GTPases are indispensable for cell growth in *Bacillus subtilis*, the HflX homolog YnbA is not.[19] The *hflX* gene is non-essential in *E. coli*[9] and *Corynebacterium glutamicum* [20] as well, and no phenotype of the knockout mutants has been described thus far.

To gain insight into the function of the HflX GTPase family, we have determined the crystal structures of the GTPase from the hyperthermo-

Grant sponsor: KNAW (NL-China Exchange program); Grant number: 04CDP006; Grant sponsor: NWO; Grant numbers: ALW-Vici project 865.05.001, ALW-Veni project 863.08.014.
†Hao Wu, Lei Sun, and Fabian Blombach contributed equally to this work.
*Correspondence to: John van der Oost, Laboratory of Microbiology, Wageningen University, Dreijenplein 10, 6703 HB Wageningen, The Netherlands. E-mail: john.vanderoost@wur.nl.
Received 28 May 2009; Revised 19 August 2009; Accepted 21 August 2009
Published online 27 August 2009 in Wiley InterScience (www.interscience.wiley.com).
DOI: 10.1002/prot.22599

philic archaeon *Sulfolobus solfataricus* (SsGBP) in the apo- and the GDP-bound forms. SsGBP appears to be a slow GTPase that contains a novel N-terminal domain termed HflX domain and a canonical G-domain at the C-terminus. The HflX domain influences GTP hydrolysis at the G-domain.

MATERIALS AND METHODS

Gene cloning, protein production, and analysis

Recombinant SsGBP was produced as described.[21] The N-terminal deletion mutant gene (*ssgbp-g*) was obtained by PCR amplification of the 3′ fragment of gene *Sso0269* coding for amino acids 176-356 using primers 5′-GCGCTCATGAGAAATAATATTCCTTCTATCGG-3′ and 5′-CGCGCCTCGAGACTCAACTGAGTTGCTAGCTGG-3′. The C-terminal deletion mutant gene (*ssgbp-h*) was obtained by PCR amplification of the 5′ fragment of *Sso0269* coding for amino acids 1–175 using primers 5′-GCGCGCTCATGAAAACAGCTGCTCTTTTTGTATC-3′ and 5′-GCGCGCTCGAGCTTATTAGATTCTATGGATTTTTC-3′. The amplification products were cloned into vector pET24d (Novagen) resulting in a C-terminal His-tag fusion protein. Expression and purification of SsGBP-G and SsGBP-H was performed as described for the full-length protein.[21]

Crystallization, data collection, and structure determination

SsGBP was crystallized as described elsewhere.[21] Apo-enyzme SsGBP crystals were soaked in 85 m*M* GDP and 10 m*M* $MgCl_2$ for 21 days to obtain the SsGBP-GDP complex crystals. Single-Wavelength Anomalous Diffraction data to 2.0 Å resolution were collected from the apo-enzyme SsGBP crystal and the SsGBP–GDP complex crystal. The structure of apo-SsGBP was solved by cadmium-based Single-wavelength Anomalous Diffraction phasing. Four Cd^{2+} ions from the reservoir solution were identified by SHELXD, giving a figure of merit of 0.51. AutoSHARP[22] was used for heavy atom refinement and phasing. To improve the quality of the electron density maps, we used SOLOMON,[23] run within autoSHARP, to perform a density modification based on solvent flattening. Approximately 80% of the polypeptide chain was built automatically using Arp/Warp.[24] The $Fo-Fc$ difference *Fourier* electron density map and omit density map displayed clear density and were used to assign the sulfate group and the two acetic acid groups. The structure was then manually rebuilt in Coot[25] and refined using CNS[26] and REFMAC.[27] The model was refined to a final R_{work} = 19.8% and R_{free} = 23.5%. The structure of the SsGBP-GDP complex was resolved in the same way. The $Fo-Fc$ difference map and omit map showed clear electron density at the guanine-nucleotide binding site into which a GDP molecule was manually docked. The model was refined to a final R_{work} = 22.7% and R_{free} = 26.2%.

Table I
Statistics of Diffraction Data and Structure Refinement of SsGBP

	Apo-SsGBP	SsGBP-GDP complex
Data collection		
Wavelength (Å)	1.5408	1.5408
Space group	$P2_12_12_1$	$P2_12_12_1$
Unit cell (Å) a, b, c	65.1, 72.6, 95.9	65.0, 72.4, 96.0
Resolution (Å)	50.0−2.00 (2.07–2.00)[a]	50.0−2.0 (2.07–2.00)
Unique reflections	30,618 (2794)	30,589 (2945)
Completeness	97.1 (89.6)	97.1 (94.3)
R_{merge}[b]	0.076 (0.256)	0.070 (0.451)
$<I/\sigma(I)>$	29.9 (9.5)	16.1 (4.6)
Redundancy	13.8 (14.0)	6.7 (6.2)
Refinement		
Resolution range	30−2.0	20−2.0
R_{work}/ R_{free}[b] (%)	19.8/23.5	22.7/26.2
RMS deviation		
bonds (Å)	0.017	0.020
angles (°)	1.41	1.68
Average B factor (Å^2):		
Protein	30.0	34.1
Water	35.8	39.1
Metal ions	34.5	36.3
Other ligands	35.1	42.6
Ramachandran plot		
Favored (%)	94.3	94.3
Allowed (%)	5.0	5.0
Generously (%)	0.4	0.4
Disallowed (%)	0.4	0.4

[a]Numbers in parentheses are corresponding values in the highest resolution shell.
[b]$R_{work} = \Sigma(\|F_p(obs)|-|F_p(calc)\|)/\ \Sigma|F_p\ (obs)|$; $R_{free} = R$ factor for a selected subset (5%) of the reflections that was not included in prior refinement calculations.
[c]$R_{merge} = \Sigma_h\Sigma_l\ |I_{hl}-<I_h>|/\Sigma_h\ \Sigma_l\ <I_h>$, where I_l is the *l*th observation of reflection *h* and $<I_h>$ is the weighted average intensity for all observations *l* of reflection *h*.

Both the final models consist of 311 residues, with residues 123–143, 166–178, and 203–213 having no interpretable density. The stereochemistry of the structure was analyzed with the program PROCHECK.[28] Both models have 94.3% of their residues in the most favored regions. In both models, Y42 is located in the disallowed region of the Ramachandran plot. Statistics of the data collection and refinement are summarized in Table I.

The atomic coordinates and structure factors of SsGBP and SsGBP-GDP complex have been deposited in the RCSB Protein Data Bank with PDB accession codes 2QTF and 2QTH, respectively.

Structural homology searches

Structural homology searches for SsGBP as well as for the separate domains were carried out with DaliLite v.3. Significant similarities were defined as recommended.[29]

Native electrospray ionization mass spectrometry

The SsGBP buffer was exchanged sequentially to 50 m*M* ammonium acetate (pH 6.8) using centrifugal filter units with a cut-off of 5 kDa (Millipore). The final protein concentration was 10 μ*M*. Samples were analyzed on an LCT electrospray time-of-flight mass-spectrometer. (Waters, Manchester, UK). Nanospray glass capillaries were used to introduce the samples into the Z-spray source. Source pressure was increased to 10 mbar to create increased collisional cooling.[30,31] Source temperature was set at 80°C and sample cone voltage was varied from 80 V to 125 V. Needle voltage was around 1300 V.

Thin layer chromatography

For Thin layer chromatography, SsGBP (8 μ*M*), SsGBP-H (8.6 μ*M*), and SsGBP-G (9.9 μ*M*) were incubated with 4.5 μ*M* of [α-^{32}P]-GTP (400 Ci/mmol, Amersham) in 50 m*M* HEPES/KOH (pH 7.7); 200 m*M* KCl; 10 m*M* $MgCl_2$) at 50°C for 20 min. Reactions were quenched with 1 volume stop buffer (2% SDS, 5 m*M* EDTA). One microliter of the reaction mixture was spotted onto 20 × 20 cm^2 PEI cellulose F plates (Merck). The plate was developed in 1*M* acetic acid, 0.8*M* LiCl. Calf Intestinal Alkaline Phosphatase (New England Biolabs) was used to produce inorganic phosphate as standard.

Phosphate release assay

GTP hydrolysis by SsGBP was measured using a malachite-green assay[32] with the following modifications. All measurements were performed in 20 m*M* Tris/HCl (pH 7.8); 200 m*M* NaCl, 5 m*M* $MgCl_2$, 5% glycerol in a total volume of 50 μL. Absorption was measured at 690 nm in a microplate reader (iEMS Reader MF. Labsystems). SsGBP and SsGBP-G samples were incubated at 50°C for 45 min and 15 min, respectively, to compensate for the lower activity of full-length SsGBP. Phosphate release was linear during these time intervals. The concentration of SsGBP-G was 0.28 μ*M* (0–100 μ*M* GTP) or 1.38 μ*M* (100–1000 μ*M* GTP), and the concentration of SsGBP was 1.41 μ*M*. Measurements were performed at least in triplicates. Values were corrected for background determined from controls without protein and controls without GTP. Inorganic phosphate concentrations were calculated using a phosphate standard in assay buffer ranging from 0 to 50 μ*M* phosphate.

RESULTS

Overall structure

The SsGBP monomer comprises 356 amino acids, and the structure displays a two domain architecture. The protein consists of a prototypical N-terminal domain (denoted HflX domain, residues 1–178) and a canonical C-terminal GTPase domain (G-domain, residues 179–356) [Fig. 1(A,B)]. The structures of apo-SsGBP and SsGBP-GDP are identical within experimental error (RMSD 0.3 Å for all 311 Cα atoms). In contrast to most other HflX GTPases, such as the *E. coli* HflX and the human homolog PGPL, SsGBP lacks the relatively poorly conserved 50 amino acid extension at the C-terminus, and therefore represents a minimal size variant within the HflX family (see Fig. 2). Native mass spectrometry revealed that SsGBP is a monomer in solution with a mass of 41604.9 ± 1 Da (theoretical mass 41603 Da), which corresponds to the monomer observed in the crystallography asymmetric unit. SsGBP remained in the monomeric state after incubation with different nucleotides (GMP, GDP, GTP, GppNHp).

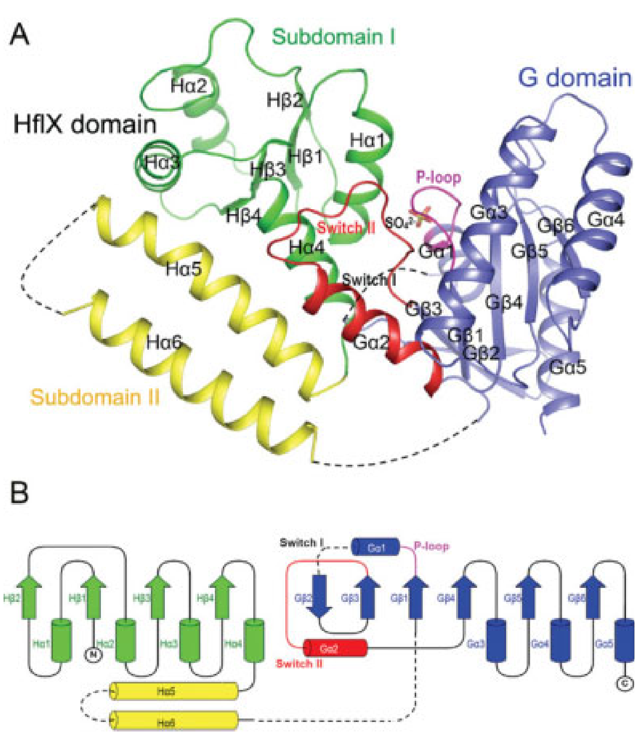

Figure 1

Overall structure of SsGBP. **A**: Ribbon representation of the SsGBP structure. Three domains are distinguished: HflX subdomain I (residues 1–99, green), HflX subdomain II (residues 100–165, yellow), and G-domain (residues 179–356, blue). The latter contains the P-loop region (magenta) and the switch II region (red). **B:** Topology diagram of SsGBP showing the connectivity of secondary structure elements and domain organization.

HflX domain

The HflX domain can be subdivided into two parts. Residues 1–99 (subdomain I) form a four-stranded parallel β-sheet (Hβ1–4) flanked by two α-helices on either side (Hα1–4). Residues 100–178 (subdomain II) make up an anti-parallel coiled coil of two long α-helices (Hα5-6) that connect the HflX domain to the G-domain [Fig. 1(A)]. The connecting stretch of amino acids

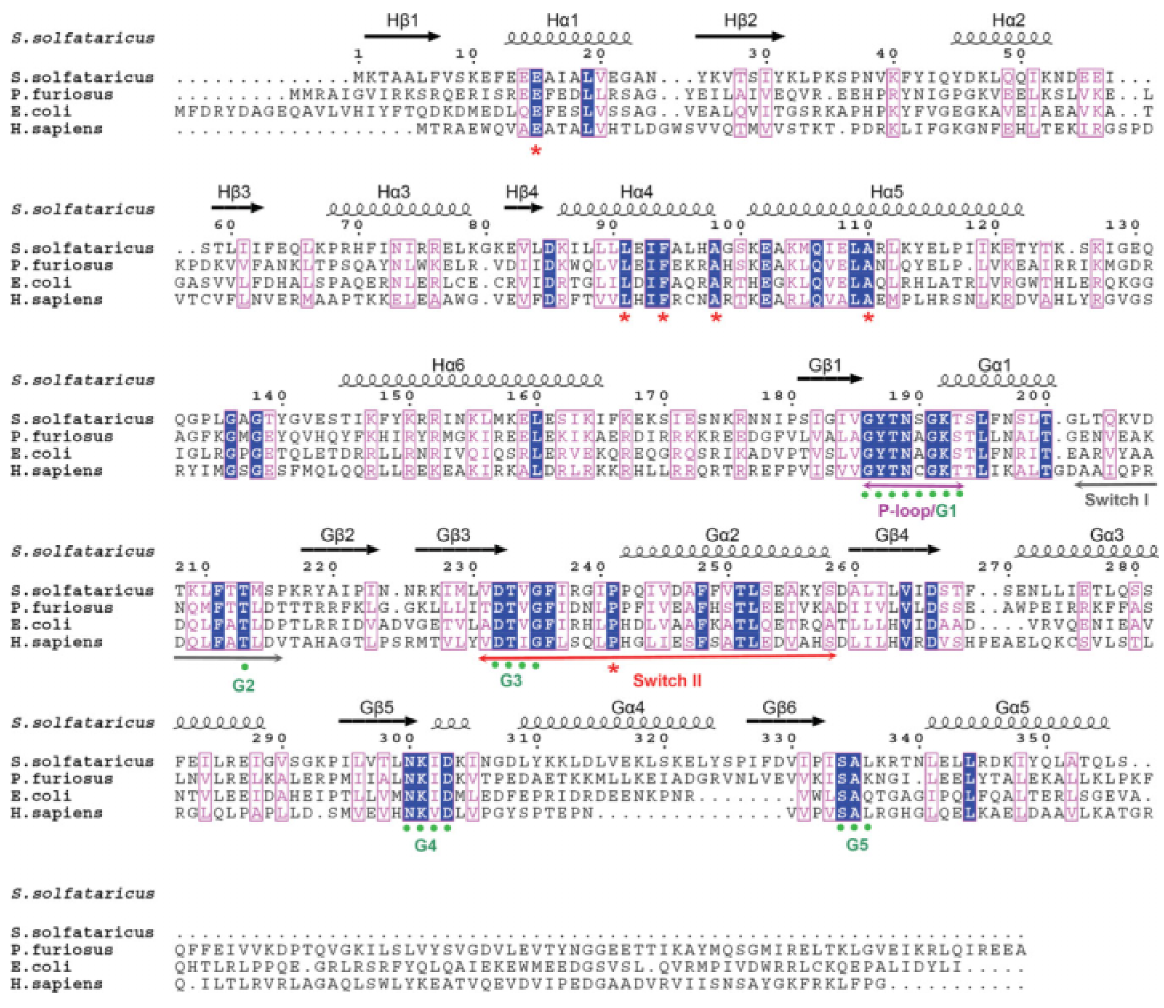

Figure 2

Sequence conservation of HflX family. Sequence alignment of SsGBP from *S. solfataricus* (gi:15897212) and homologs from *Pyrococcus furiosus* (gi:18977549), *Escherichia coli* (gi:16131995), and *Homo sapiens* (gi:6912588). Identical and similar residues are highlighted in blue and purple, respectively. Identical residues involved in domain interaction are marked by red asterisks. The guanine nucleotide binding motifs (G1–G5), the P-loop, and the switch regions are indicated.

(residues 166–178) that links the domains was disordered in both the apo and GDP-bound structure, which reflects a structural flexibility in this region, allowing possible domain rearrangements.

The only other disordered region of the HflX domain (residues Y123-E143) links the two long α-helices (Hα5-6) of subdomain II. In many HflX homologs this linker region contains several glycines (see Fig. 2),[3,10] which may contribute to the structural flexibility of this 20-amino acid loop. The pair of α-helices (Hα5-6) is held together mostly by hydrophobic interactions mediated by residues M105, L109, L112, L116, and I119 from Hα5 and I146, Y149, I153, L156, and L160 from Hα6, and by a conserved ion pair between E108 and R152. Interestingly, many positively charged residues are present in Hα5 (K101, K104, K113, and K120) and Hα6 (K147, K150, R151, R152, K155, and K164). Together with R69 from Hα3 they form a positively charged patch at the surface of the HflX-domain (see Fig. 3).

G-domain

The G-domain of SsGBP is composed of six β-strands (Gβ1(Gβ6) and five α-helices (Gα1(Gα5) (see Fig. 1). The five nucleotide-binding motifs characteristic for the G-domain are present in *S. solfataricus* HflX (see Fig. 2): Gx_4GKS/T (G1-motif, or P-loop), T (G2-motif), Dx_2G (G3-motif), N/TKxD (G4-motif), and SAK/L (G5-motif).[1,3] In the GDP-bound SsGBP structure, the GDP molecule is bound by residues in the P-loop (G1: N189, S190, K192, G191, T193, and S194), the switch II region (G3: D232 and T233), the G4-motif (N300 and K301), and the G5-motif (S334, A335, and L336) (see Fig. 4).

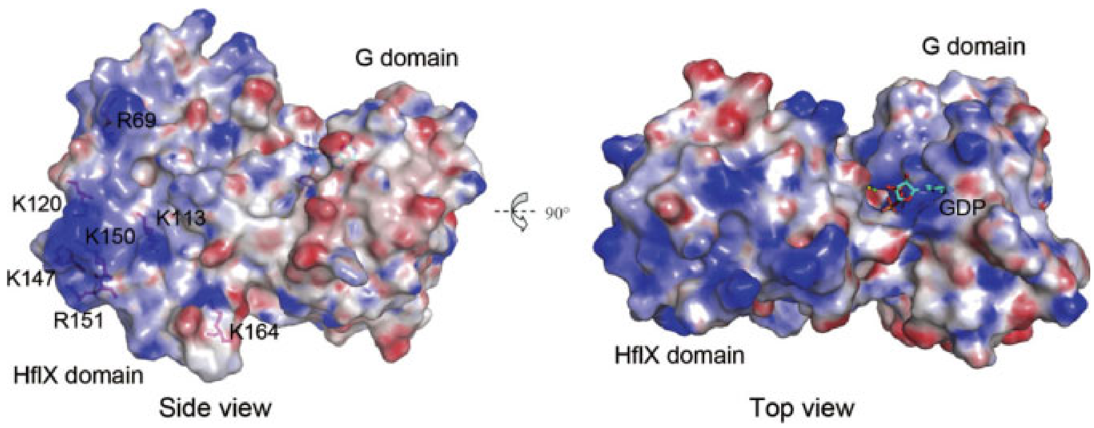

Figure 3

Electrostatic surface (−15 to 15 kT.e^{-1}) of SsGBP-GDP complex. Residues contributing to the highly positively charged site of the HflX domain are shown in a ball-and-stick representation.

S243 and N349 in *C. pneumoniae* HflX, corresponding to T193 and N300 in SsGBP, respectively, are essential for intrinsic GTPase activity.[11] As in many other GTPase structures,[33–35] a large part of switch I (T203 to T213) was disordered in both the apo and the GDP bound structures of SsGBP. A Mg^{2+} ion was present in the nucleotide binding pocket of the GDP-bound structure. The Mg^{2+} ion is coordinated by T193 (G1) and an oxygen atom from the β-phosphate group of GDP, and an aspartate residue from switch II (D232) through a water molecule. This coordination corresponds to the described Mg^{2+} ion binding mode of GTPases in complex with GDP or GTP analogs.[36] However, the switch II aspartate usually coordinates the the Mg^{2+} ion directly. The additional water molecule between D232 and the Mg^{2+} ion positions the the Mg^{2+} ion closer to the P-loop

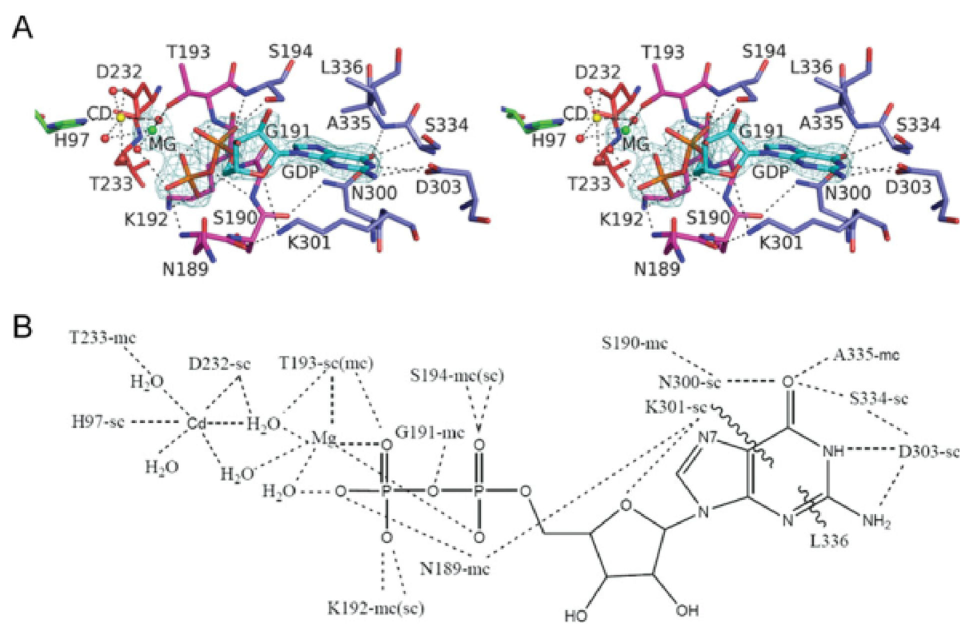

Figure 4

GDP binding site of SsGBP. **A**: Stereo view of the Guanine nucleotide binding site. Dashed lines indicate potential hydrogen bonds. The superimposed (2*Fo*−*Fc*) electron density map was calculated with the GDP omitted from phasing and was contoured at 1.0σ with a 2.0-Å cover radius. Red balls indicate water molecules bound to GDP-Mg^{2+} or Cd^{2+}. **B**: Schematic diagram showing the hydrogen bonding interactions between SsGBP and GDP-Mg^{2+}. An "sc" or "mc" index indicates involvement of a side-chain or main-chain atom, respectively. Waved lines symbolize stacking interactions.

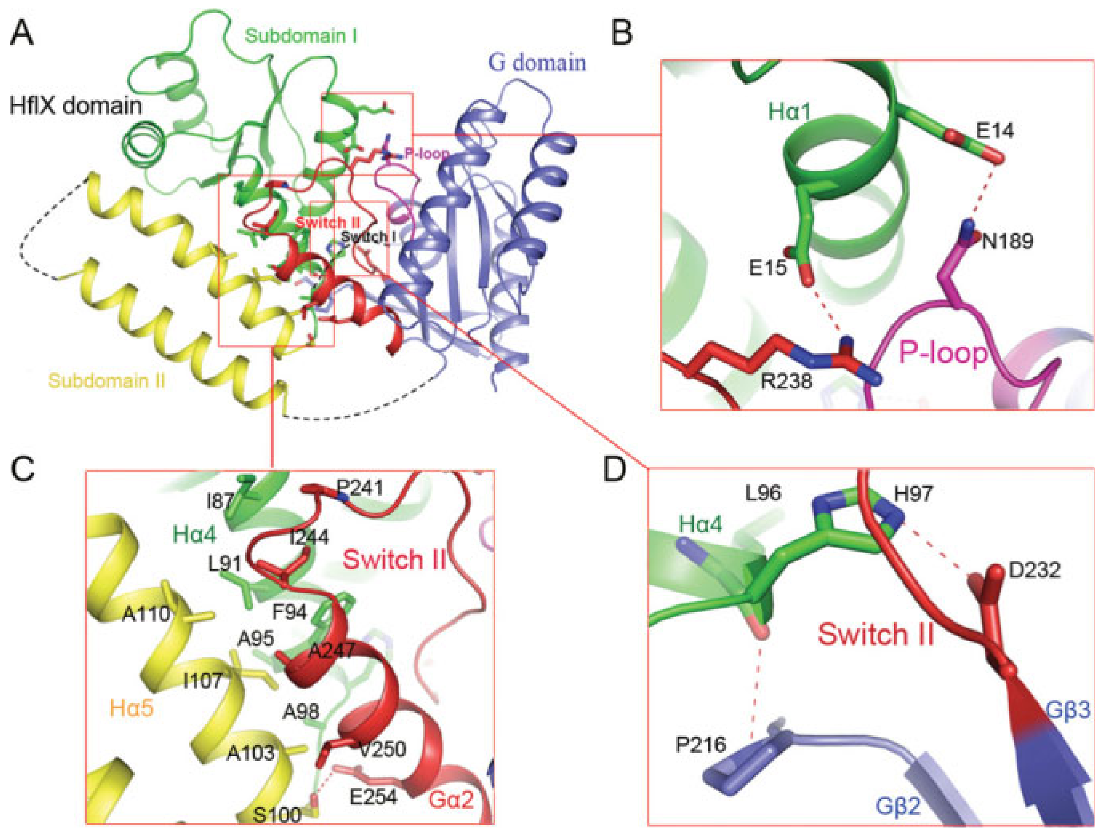

Figure 5

Interface of the HflX domain and the G-domain. **A:** Overall structure of SsGBP with side chains of residues involved in interdomain interaction. **B:** Interaction between Hα1 and G-domain. The dashed lines indicate hydrogen bonds and salt bridges. **C:** Interaction between Hα4, Hα5, and Gα2. S100 and E254 form a hydrogen bond, all the other residues are involved in hydrophobic interactions. **D:** Interaction between Hα4 and G-domain.

contacting also an oxygen atom of the α-phosphate group of GDP (3.1 Å distance).

Four Cd^{2+} ions were found in the asymmetric unit of the apo and the GDP-bound SsGBP crystals, one of which was found in the nucleotide-binding pocket [Fig. 4(A)]. In the GDP-bound structure, the Cd^{2+} ion in the nucleotide-binding pocket is located at a distance of 4.5 Å from the Mg^{2+} ion. The Cd^{2+} ion is coordinated by H97 from Hα4, D232 from switch II, and four water molecules (see Fig. 4). The Cd^{2+} ion originates from the crystallization buffer and is unlikely to be biologically significant. Strong electron density was also observed at the position corresponding to the β-phosphate group of GDP in the apo SsGBP structure. This density was interpreted as a sulfate ion from the crystallization buffer. The close proximity of this Cd^{2+} ion to the Mg^{2+} ion could potentially influence the position of the latter one.

Domain interface

The HflX and the G-domain of SsGBP have an extensive interface in which the GTP binding site resides. The two domains bury a total of 1870 Å^2 solvent accessible surface area in the GDP-bound SsGBP structure (calculated using a 1.4 Å probe). Contacts between the domains are mediated by the structural elements Hα1, Hα4, and Hα5 of the HflX domain, and the P-loop and the switch II region of the G-domain (see Fig. 5). Hα1 interacts with the P-loop and switch II by a hydrogen bond (E14-N189) and a salt bridge (E15-R238), respectively [Fig. 5(B)]. Hα4 and Hα5 form a three α-helix bundle with Gα2 of switch II [Fig. 5(C)]. Furthermore D232 in the switch II region forms a hydrogen bond with H97 in Hα4 [Fig. 5(D)]. Some of the residues involved in the domain interaction are completely conserved within the HflX family, such as E15, L91, F94, A98, A110, and N189 (see Fig. 2) indicating that the inter-domain contact is a conserved feature of HflX GTPases.

Interactions between HflX and G-domain reduce GTPase activity

Intrinsic GTPase activity has previously been reported for *E. coli* HflX[9] and its homolog in *C. pneumoniae*.[11] GTP hydrolysis was detected for SsGBP as well as an

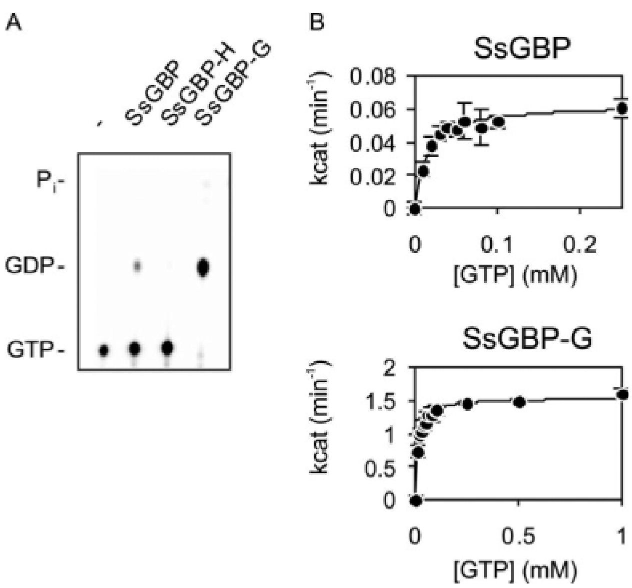

Figure 6

GTP hydrolysis. **A:** GTPase activity of full-length SsGBP, the G-domain deletion mutant (SsGBP-H), and the N-terminal deletion mutant (SsGBP-G) as detected by thin layer chromatography using [α-^{32}P]-GTP. **B:** Substrate dependent activity at 50°C of SsGBP and SsGBP-G measured by phosphate release assays. Error bars represent ×1 standard deviation.

N-terminal deletion mutant (SsGBP-G), but not a G-domain deletion mutant (SsGBP-H), confirming that the detected GTPase activity for SsGBP and SsGBP-G was not due to phosphatase contamination [Fig. 6(A)]. A wide range of GTP concentrations was further tested in Phosphate-release assays. The k_{cat} value for full-length SsGBP was 0.063 ± 0.002 min^{-1} and the K_m value 14.1 ± 2.0 μ*M*, showing that SsGBP is a slow GTPase with relatively low affinity for GTP. SsGBP-G displayed a similar K_m value (12.9 ± 0.8 μ*M*), whereas the substrate turnover rate k_{cat} was 24-fold increased (1.54 ± 0.01 min^{-1}) [Fig. 6(B)], indicating a reduction of activity of the G-domain by the HflX domain in the full-length SsGBP.

DISCUSSION

HflX GTPases belong to the TRAFAC class of GTPases, and are widely distributed in the three domains of life.[3,5] Despite their ubiquitous occurrence, the physiological function of this class of proteins is relatively poorly understood. SsGBP is a monomeric protein like its *E. coli* homologue HflX[9] and its structure displays two domains as has been predicted.[3] The structure of the C-terminal G-domain closely resembles that of many well-characterized GTPases such as GDP-bound human Ras (PDB:ID 4Q21, RMSD 2.8 Å) (Milburn *et al.*, 1990). Structural homology searches for the N-terminal HflX domain on the other hand revealed only weak similarity to structures in the protein databank. The positively charged patch at the surface of the HflX domain suggests that HflX GTPases interact with nucleic acids. The strict conservation of several residues that make up the positive patch (K104, K147, K150 and R152) shows that this is an important structural feature of the HflX family. Recent studies have shown that the *E. coli* and *C. pneumoniae* HflX associate with the 50S ribosomal subunit.[10,11] We therefore hypothesize that the HflX domain interacts with ribosomal RNA via the positive patch. In contrast to the majority of TRAFAC GTPases that interact with the ribosome, the binding of *E. coli* HflX to the large ribosomal subunit is not restricted to the active state.[10] This is consistent with the observation that the archaeal homolog SsGBP exposes the positively charged patch in the inactive state. Similar to *E. coli* HflX, SsGBP binds to the 50S ribosomal subunit independent of the bound nucleotide (Blombach, unpublished results). In line with our hypothesis the HflX-domain is required for ribosome binding by *E. coli* HflX.[10] RNA-binding domains are a common feature of many TRAFAC GTPases involved in ribosome assembly or biogenesis, but unlike the G-domain, the RNA-binding domains generally belong to a variety of protein families. The Obg family for instance contains two types of RNA-binding domains: TGS in *H. influenza* YchF[37] and OCT in *Thermus thermophilus* Obg.[38] Our structural data suggest that the HflX-domain likely constitutes a new type of RNA-binding domain.

The switch I region of SsGBP is disordered in both the nucleotide-free and the GDP-bound forms. Similar structural flexibility is observed in many other GTPase structures such as *T. thermophilus* elongation factor G.[39,40] Together with switch II, the switch I region of the G-domain is known to change conformation upon binding GTP, exerting the "molecular switch" function of the G-domain and setting it in the active state. In some multi-domain GTPases, this conformational change is thought to trigger further protein rearrangements driving a biological process. Structures of several other GTPases such as Obg,[41] Era[42] and EngA[34] have revealed that switch I- and II-mediated interdomain interactions are a common theme. For instance, EngA is thought to undergo conformational changes upon GTP-binding, affecting the relative position of the domains, thereby controlling its interaction with RNA.[34] The switch II region of the N-terminal G-domain of EngA appears to play a central role in this transition. Although we did not obtain the SsGBP crystal structure in its GTP bound state, we speculate that rearrangements of both switch I and II could reposition the HflX domain. While the switch regions can adopt various conformations in the GDP-bound state, their position in the GTP-bound state is usually very similar.[2] Given the inter-domain location of the switch regions in SsGBP, this conformation would require the domains to move away from each other, a process in which the flexible linker could act as a hinge. Such structural rearrangement might regulate ligand interactions of HflX.

Current models about the function of GTPases include the recruitment of extrinsic factors to ribosomal subunits, where the ribosome acts as effector of the GTPase, that is the GTPase binds with higher affinity in its active state.[4] Given the nucleotide-independent interaction of HflX with the large ribosomal subunit,[10,11] GTP hydrolysis might be used regulate the interaction with an effector such as an extrinsic factor involved for example in ribosome biogenesis. The stimulation of GTPase activity by the large ribosomal subunit as observed for *E. coli* HflX[10,11] would ensure release of the effector when it has been delivered to the ribosomal subunit. Binding of the translation elongation factors EF-Tu and EF-G to the ribosome causes repositioning of mobile elements that are critical for GTP hydrolysis.[43,44] In EF-G, these rearrangements involve the interface of its G-domain and domain III.[43] In SsGBP, the domain interface includes switch II and the P-loop. Binding of the ribosome or a ribonucleoprotein complex to SsGBP might similarly lead to structural rearrangements in SsGBP favoring GTP hydrolysis. Interestingly, the interdomain interactions of SsGBP reduce GTP hydrolysis at the G-domain and may provide control mechanism, possibly by holding switch II in a conformation that is unfavorable for GTP-hydrolysis.

ACKNOWLEDGMENTS

The authors gratefully acknowledge Dr. Zhiyong Lou (Laboratory of Structural Biology, Tsinghua University, Beijing) for the X-ray data collection of SsGBP-GDP.

REFERENCES

1. Bourne HR, Sanders DA, McCormick F. The GTPase superfamily: a conserved switch for diverse cell functions. Nature 1990;348:125–132.
2. Vetter IR, Wittinghofer A. The guanine nucleotide-binding switch in three dimensions. Science 2001;294:1299–1304.
3. Leipe DD, Wolf YI, Koonin EV, Aravind L. Classification and evolution of P-loop GTPases and related ATPases. J Mol Biol 2002;317:41–72.
4. Karbstein K. Role of GTPases in ribosome assembly. Biopolymers 2007;87:1–11.
5. Caldon CE, March PE. Function of the universally conserved bacterial GTPases. Curr Opin Microbiol 2003;6:135–139.
6. Bourne HR, Sanders DA, McCormick F. The GTPase superfamily: conserved structure and molecular mechanism. Nature 1991;349:117–127.
7. Gianfrancesco F, Esposito T, Montanini L, Ciccodicola A, Mumm S, Mazzarella R, Rao E, Giglio S, Rappold G, Forabosco A. A novel pseudoautosomal gene encoding a putative GTP-binding protein resides in the vicinity of the Xp/Yp telomere. Hum Mol Genet 1998;7:407–414.
8. Noble JA, Innis MA, Koonin EV, Rudd KE, Banuett F, Herskowitz I. The *Escherichia coli* hflA locus encodes a putative GTP-binding protein and two membrane proteins, one of which contains a protease-like domain. Proc Natl Acad Sci USA 1993;90:10866–10870.
9. Dutta D, Bandyopadhyay K, Datta AB, Sardesai AA, Parrack P. Properties of HflX, an enigmatic protein from *Escherichia coli*. J Bacteriol 2009;191:2307–2314.
10. Jain N, Dhimole N, Khan AR, De D, Tomar SK, Sajish M, Dutta D, Parrack P, Prakash B. E. coli HflX interacts with 50S ribosomal subunits in presence of nucleotides. Biochem Biophys Res Commun 2009;379:201–205.
11. Polkinghorne A, Ziegler U, Gonzalez-Hernandez Y, Pospischil A, Timms P, Vaughan L. *Chlamydophila pneumoniae* HflX belongs to an uncharacterized family of conserved GTPases and associates with the *Escherichia coli* 50S large ribosomal subunit. Microbiology 2008;154 (Part 11):3537–3546.
12. Sayed A, Matsuyama S, Inouye M. Era, an essential *Escherichia coli* small G-protein, binds to the 30S ribosomal subunit. Biochem Biophys Res Commun 1999;264:51–54.
13. Sharma MR, Barat C, Wilson DN, Booth TM, Kawazoe M, Hori-Takemoto C, Shirouzu M, Yokoyama S, Fucini P, Agrawal RK. Interaction of Era with the 30S ribosomal subunit implications for 30S subunit assembly. Mol Cell 2005;18:319–329.
14. Wout P, Pu K, Sullivan SM, Reese V, Zhou S, Lin B, Maddock JR. The *Escherichia coli* GTPase CgtAE cofractionates with the 50S ribosomal subunit and interacts with SpoT, a ppGpp synthetase/hydrolase. J Bacteriol 2004;186:5249–5257.
15. Zhang S, Haldenwang WG. Guanine nucleotides stabilize the binding of *Bacillus subtilis* Obg to ribosomes. Biochem Biophys Res Commun 2004;322:565–569.
16. Uicker WC, Schaefer L, Britton RA. The essential GTPase RbgA (YlqF) is required for 50S ribosome assembly in *Bacillus subtilis*. Mol Microbiol 2006;59:528–540.
17. Schaefer L, Uicker WC, Wicker-Planquart C, Foucher AE, Jault JM, Britton RA. Multiple GTPases participate in the assembly of the large ribosomal subunit in *Bacillus subtilis*. J Bacteriol 2006;188: 8252–8258.
18. Wicker-Planquart C, Foucher AE, Louwagie M, Britton RA, Jault JM. Interactions of an essential *Bacillus subtilis* GTPase. Ysx C, with ribosomes J Bacteriol 2008;190:681–690.
19. Morimoto T, Loh PC, Hirai T, Asai K, Kobayashi K, Moriya S, Ogasawara N. Six GTP-binding proteins of the Era/Obg family are essential for cell growth in *Bacillus subtilis*. Microbiology 2002;148 (Part 11):3539–3552.
20. Engels S, Ludwig C, Schweitzer JE, Mack C, Bott M, Schaffer S. The transcriptional activator ClgR controls transcription of genes involved in proteolysis and DNA repair in *Corynebacterium glutamicum*. Mol Microbiol 2005;57:576–591.
21. Wu H, Sun L, Brouns SJ, Fu S, Akerboom J, Li X, van der Oost J. Purification, crystallization and preliminary crystallographic analysis of a GTP-binding protein from the hyperthermophilic archaeon *Sulfolobus solfataricus*. Acta Crystallograph Sect F Struct Biol Cryst Commun 2007;63 (Part 3):239–241.
22. de la Fortelle E, Bricogne G. Maximum-likelihood heavy-atom parameter refinement for multiple isomorphous replacement and multiwavelength anomalous diffraction methods. Methods Enzymol 1997;276:472–494.
23. Abrahams JP, Leslie AGW. Methods used in the structure determination of bovine mitochondrial F1 ATPase. Acta Crystallographica Section D 1996;52:30–42.
24. Perrakis A, Morris R, Lamzin VS. Automated protein model building combined with iterative structure refinement. Nat Struct Biol 1999;6:458–463.
25. Emsley P, Cowtan K. Coot: model-building tools for molecular graphics. Acta Crystallogr D Biol Crystallogr 2004;60 (Part 12 Part 1):2126–2132.
26. Brunger AT, Adams PD, Clore GM, DeLano WL, Gros P, Grosse-Kunstleve RW, Jiang JS, Kuszewski J, Nilges M, Pannu NS, Read RJ, Rice LM, Simonson T, Warren GL. Crystallography and NMR system: a new software suite for macromolecular structure determi-

nation. Acta Crystallogr D Biol Crystallogr 1998;54 (Part 5):905–921.
27. Murshudov GN, Vagin AA, Dodson EJ. Refinement of macromolecular structures by the maximum-likelihood method. Acta Crystallogr D Biol Crystallogr 1997;53 (Part 3):240–255.
28. Laskowski RA, MacArthur MW, Moss DS, Thornton JM. PROCHECK: a program to check the stereochemical quality of protein structures. J Appl Crystallogr 1993;26:283–291.
29. Holm L, Kaariainen S, Rosenstrom P, Schenkel A. Searching protein structure databases with DaliLite v. 3. Bioinformatics 2008;24:2780–2781.
30. Krutchinsky AN, Chernushevich IV, Spicer VL, Ens W, Standing KG. Collisional damping interface for an electrospray ionization time-of-flight mass spectrometer. J Am Soc Mass Spectr 1998; 9:569–579.
31. Tahallah N, Pinske M, Maier CS, Heck AJ. The effect of the source pressure on the abundance of ions of noncovalent protein assemblies in an electrospray ionization orthogonal time-of-flight instrument. Rapid Commun Mass Spectr 2001;15:596–601.
32. Esue O, Cordero M, Wirtz D, Tseng Y. The assembly of MreB, a prokaryotic homolog of actin. J Biol Chem 2005;280:2628–2635.
33. Constantinescu AT, Rak A, Alexandrov K, Esters H, Goody RS, Scheidig AJ. Rab-subfamily-specific regions of Ypt7p are structurally different from other RabGTPases. Structure 2002;10:569–579.
34. Muench SP, Xu L, Sedelnikova SE, Rice DW. The essential GTPase YphC displays a major domain rearrangement associated with nucleotide binding. Proc Natl Acad Sci USA 2006;103:12359–12364.
35. Robinson VL, Hwang J, Fox E, Inouye M, Stock AM. Domain arrangement of Der, a switch protein containing two GTPase domains. Structure 2002;10:1649–1658.
36. Ruzheinikov SN, Das SK, Sedelnikova SE, Baker PJ, Artymiuk PJ, Garcia-Lara J, Foster SJ, Rice DW. Analysis of the open and closed conformations of the GTP-binding protein YsxC from *Bacillus subtilis*. J Mol Biol 2004;339:265–278.
37. Teplyakov A, Obmolova G, Chu SY, Toedt J, Eisenstein E, Howard AJ, Gilliland GL. Crystal structure of the YchF protein reveals binding sites for GTP and nucleic acid. J Bacteriol 2003;185:4031–4037.
38. Kukimoto-Niino M, Murayama K, Inoue M, Terada T, Tame JR, Kuramitsu S, Shirouzu M, Yokoyama S. Crystal structure of the GTP-binding protein Obg from Thermus thermophilus HB8. J Mol Biol 2004;337:761–770.
39. Aevarsson A, Brazhnikov E, Garber M, Zheltonosova J, Chirgadze Y, al-Karadaghi S, Svensson LA, Liljas A. Three-dimensional structure of the ribosomal translocase: elongation factor G from *Thermus thermophilus*. Embo J 1994;13:3669–3677.
40. Czworkowski J, Wang J, Steitz TA, Moore PB. The crystal structure of elongation factor G complexed with GDP, at 2.7 A resolution. Embo J 1994;13:3661–3668.
41. Buglino J, Shen V, Hakimian P, Lima CD. Structural and biochemical analysis of the Obg GTP binding protein. Structure 2002;10: 1581–1592.
42. Chen X, Court DL, Ji X. Crystal structure of ERA: a GTPase-dependent cell cycle regulator containing an RNA binding motif. Proc Natl Acad Sci USA 1999;96:8396–8401.
43. Connell SR, Takemoto C, Wilson DN, Wang H, Murayama K, Terada T, Shirouzu M, Rost M, Schuler M, Giesebrecht J, Dabrowski M, Mielke T, Fucini P, Yokoyama S, Spahn CM. Structural basis for interaction of the ribosome with the switch regions of GTP-bound elongation factors. Mol Cell 2007;25:751–764.
44. Villa E, Sengupta J, Trabuco LG, LeBarron J, Baxter WT, Shaikh TR, Grassucci RA, Nissen P, Ehrenberg M, Schulten K, Frank J. Ribosome-induced changes in elongation factor Tu conformation control GTP hydrolysis. Proc Natl Acad Sci USA 2009;106:1063–1068.